

Longitudinal Observation of Retinal Response to Optic Nerve Transection in Rats Using Visible Light Optical Coherence Tomography

Shaohua Pi, Bingjie Wang, Min Gao, William Cepurna, Diana C. Lozano, John C. Morrison, and Yali Jia

Casey Eye Institute, Oregon Health & Science University, Portland, Oregon, United States

Correspondence: Yali Jia, Casey Eye Institute, Oregon Health & Science University, Portland, OR 97239, USA; jiaya@ohsu.edu.

Received: December 30, 2022

Accepted: March 14, 2023

Published: April 14, 2023

Citation: Pi S, Wang B, Gao M, et al. Longitudinal observation of retinal response to optic nerve transection in rats using visible light optical coherence tomography. *Invest Ophthalmol Vis Sci.* 2023;64(4):17. <https://doi.org/10.1167/iovs.64.4.17>

PURPOSE. To characterize rat retinal responses after optic nerve transection (ONT) by visible-light optical coherence tomography (vis-OCT).

METHODS. Unilateral ONT was performed in Brown Norway rats ($n = 8$). In vivo, vis-OCT retinal imaging was performed on the experimental eyes before ONT (baseline), and two days, one week, two weeks, and four weeks (endpoint) after ONT, as well as on fellow eyes at the endpoint. The system was operated at a 70 kHz A-line sampling rate with both raster scans ($512 \times 2 \times 512$ A-lines), and circular scans (2048×100 A-lines) acquired around the optic disc. Retinal layers were segmented to calculate layer thicknesses and project en face images for visualization and quantifications. Vessel densities and oxygen saturation were used to evaluate the morphologic and functional impact on the retinal vasculature.

RESULTS. After ONT, retinal nerve fiber bundles demonstrated significant degeneration, starting at two weeks, with a reduction of thicknesses quantified on the nerve fiber layer, ganglion cell complex, and total retina. Along with that, the activation of macrophage-like cells in the vitreoretinal interface was also observed. Vessel densities for all three retinal plexuses were unaffected over the period of observation. However, oxygen saturation in retinal arteries and veins was significantly reduced at four weeks after ONT.

CONCLUSIONS. Vis-OCT can provide high-definition, in vivo characterization of retinal responses to ONT in rats. Despite a significant reduction in retinal layer thickness, this was not accompanied by alterations in vascular density. Despite this, oximetry indicates reduced retinal oxygen saturation, suggesting that altered vascular physiology is not reflected in the anatomic appearance of retinal blood vessel density alone.

Keywords: optic nerve transection, visible light OCT, glaucoma, neurodegeneration, oxygen saturation

G laucoma is a significant cause of blindness globally.¹ Clinically, glaucoma patients exhibit retinal neurodegeneration² and vascular impairment.³ Among the various animal models available for studying glaucomatous optic nerve injury,⁴ optic nerve transection (ONT)^{5,6} in rodents represents an acute and traumatic model that reliably produces significant retinal neurodegeneration caused by axonal injury. However, although several studies show that axonal loss in human glaucoma is accompanied by a reduction of inner retinal vasculature, the effects of ONT on the retinal vasculature are less certain. Recently, an optical coherence tomography angiography (OCTA) study in mice found that loss of inner retinal layers induced by either axonal injury (ONT and optic nerve crush) or retinal ganglion cell damage (NMDA injection) does not appear to affect retinal vascular density.⁷ This finding is surprising because a diminished OCTA signal would be expected after retinal ganglion cell (RGC) loss because of reduced energy requirement. The authors speculated that the resistance of retinal perfusion could be partially explained by

the neuroinflammatory response after RGC apoptosis, thus requiring sustained oxygen supply. Although the mechanism of neurodegeneration after acute optic nerve injury may be different from that in glaucoma patients, this result warrants further assessment in the rat eye because of the popularity of ONT for studying retinal events after optic nerve axon injury, and because responses of the retinal vasculature in human glaucoma have been extensively studied.⁸⁻¹²

Visible light optical coherence tomography (vis-OCT)^{11,13-15} is an emerging imaging modality for in vivo, noninvasive, and longitudinal monitoring of the retina for both rodents^{11,14,16} and humans.¹⁷⁻²⁰ Besides high-resolution retinal structure and angiography, vis-OCT can also provide functional oxygen saturation measurement across the entire retinal vascular tree.¹³ In this study, we used vis-OCT to image rat retinas before and after ONT and characterized the neurodegenerative and vascular impairments by studying retinal layer thickness, blood vessel density, and blood oxygen saturation.



METHODS

Animal Preparation

Animal procedures complied with the Association for Research in Vision and Ophthalmology Statement for the Use of Animals in Ophthalmic and Vision Research. Ethics approval for the protocols was obtained from the Institutional Animal Care and Use Committee of the Oregon Health & Science University (OHSU). Adult brown Norway rats ($n = 8$) were used for this study. One eye of each animal was randomly chosen to undergo ONT. During imaging sessions, animals were first anesthetized with 5% isoflurane mixed with normal air (21% O_2) for 10 minutes, followed by 2.5% isoflurane to maintain anesthesia. Exhaust gas was circulated and removed by a vacuum pump connected with an anesthesia gas filter (Omnicon F/air; A.M. Bickford, Wales Center, NY, USA) before being released. The animals' pupil was dilated with a 1% tropicamide ophthalmic solution. To keep the cornea moist, sterile irrigating salt solution (Alcon Laboratories Inc., Geneva, Switzerland) was applied frequently throughout the experiments. Body temperature was maintained at 38°C with a circulating warm water blanket.

ONT Procedure

ONT was performed unilaterally in rats under 2% to 3% isoflurane anesthesia (100% oxygen, on a warm water blanket) with an aseptic technique. With the use of a binocular operating microscope, the superior conjunctiva was incised to separate the muscles and connective tissue and to expose the optic nerve through a longitudinal incision through the optic nerve sheath. With Vannas scissors, the optic nerve was transected 2 mm behind the globe, and a segment 0.5 to 1.0 mm long was removed to ensure complete transection of all nerve fibers without disturbing the inferior optic nerve sheath and blood supply to the retina. The conjunctiva was then reapposed to the limbus, and the eye dressed with

erythromycin antibiotic ointment. The retinas were examined ophthalmoscopically to ensure blood vessel patency immediately after the procedure. Buprenorphine (0.05–0.1 mg/kg subcutaneous every 8–12 hours) was used as an analgesic for two days after operation.

Imaging Acquisition and Processing

Retinal vis-OCT scans were acquired at a A-line sampling rate of 70 kHz using a prototype²¹ developed in the Center for Ophthalmic Optics & lasers at OHSU. The system covered a light spectrum from 510 nm to 610 nm from a laser (EXU-6 OCT; NKT Photonics, Boston, MA, USA), providing 1.2-μm axial resolution in tissue. The incident power on the cornea was 0.8 mW. Customized software with real-time structural and angiographic OCT visualization was used to record the interferogram for further analysis.

The scans were acquired before ONT (Baseline) and at two days, one week, two weeks, and four weeks (endpoint) after ONT. This timeline was based on published histologic evidence that only 10% of retinal ganglion cells survive at two weeks after ONT.²² For a sub-group ($n = 5$) of the animals, fellow eyes were also imaged at the endpoint to compare to the changes of experimental eyes at same time point. At each session, two imaging protocols were used to acquire the desired scans for analysis. First, volumetric raster scans consisting of $512 \times 2 \times 512$ A-lines covering a 2.2 × 2.2-mm field of view near the optic disc were acquired for angiography and oxygen saturation analysis. Second, circular scans ($r = 0.8$ mm) consisting of 2048×100 A-lines were acquired around the optic disc for retinal layer thickness analysis. The interferogram was recorded by a line scan camera and further processed in MATLAB (MathWorks, Inc., Natick, MA, USA), as previously described,²³ to resolve the retinal OCT and OCTA volumes. Retinal layers were first automatically segmented using a graph-searching method²⁴ and then manually corrected to ensure the boundary accuracy.

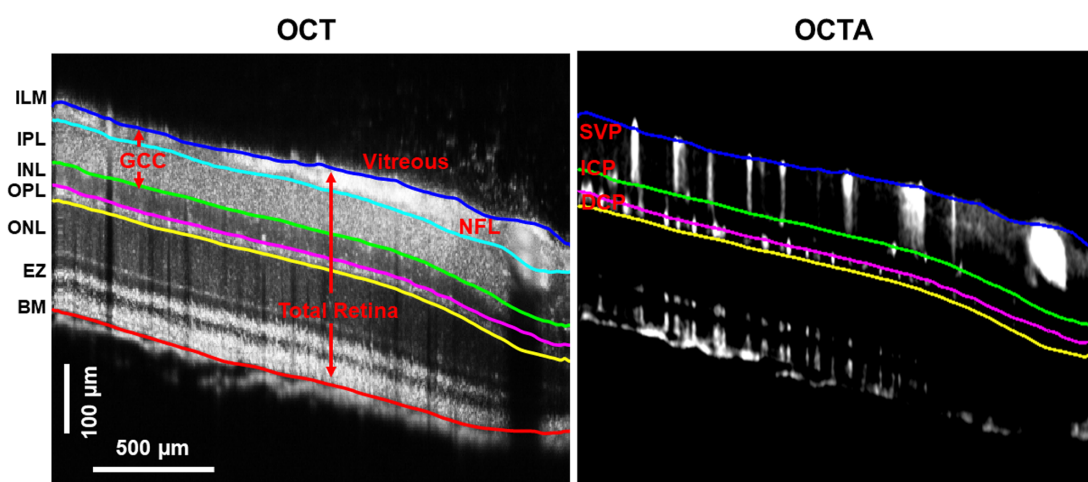


FIGURE 1. Definitions of retinal layer slabs and vascular plexuses in rats as demonstrated in OCT and OCTA B-scans. Vitreous: projected from 40 μm above inner limiting membrane (ILM, blue line) to 3 μm above ILM. NFL, projected from ILM to 25 μm below ILM for en face visualization, or from ILM to the lower boundary (cyan line) of NFL for thickness analysis. Ganglion cell complex (GCC) nerve fiber layer, defined as the slab within the ILM to the lower boundary (green line) of the inner plexiform layer (IPL). Total retina, defined as the slab between the ILM and Bruch's membrane (BM, red line). SVP, defined as the slab within the ILM to the 10 μm above the lower boundary (green line) of IPL. ICP, defined as the slab between the 3 μm above and 10 μm below the lower boundary (green line) of IPL. DCP, defined as the slab between the upper (magenta line) and lower (yellow line) boundaries of the outer plexiform layer (OPL). ONL, outer nuclear layer; EZ, ellipsoid zone. The boundaries are inclusive in the slabs.

To evaluate retinal neurodegeneration following ONT, we performed retinal layer thickness measurements on three individual slabs: nerve fiber layer (NFL), ganglion cell complex, and total retina. These slabs were segmented and analyzed on circular scans (Fig. 1). In three-dimensional OCT volumes, the NFL slab and the total retinal slab were segmented and projected on two-dimensional maps, respectively. The NFL reflectivity was quantified by relative reflectance, which was defined as the ratio of average OCT reflectance from the NFL slab to that from the total retina slab. The vitreous slab was also segmented and projected to visualize newly appeared cells or tissues after ONT surgery.²⁵ In OCTA volumes, superficial vascular plexus (SVP), intermediate capillary plexus (ICP), and deep capillary plexus (DCP) were segmented and generated for en face visualization and quantification of vessel density.^{11,21} Vessel densities, calculated as the percentage of area occupied by vascular pixels in SVP, ICP, and DCP en face angiogram images, were used to evaluate the changes in retinal vascular morphology following ONT. In the same OCTA volumes, guided by the vessel binary masks, oxygen saturation (sO_2) in blood vessels was measured using the spectroscopic fitting method.^{14,26}

A linear mixed-effect model was used to test whether ONT caused retinal damage during the longitudinal study, where the biomarkers, including retinal thickness, vessel density, and oxygen saturation, were the response vari-

ables, with the days after ONT surgery being the fixed effect (dependent variable) and the animal being the random effect. After the linear mixed-effect model test, two-sample *t*-tests were used to determine the significance ($P < 0.05$) for a specific biomarker between groups (experimental eyes to fellow eyes) and at two time points, which was performed using SPSS 23.0 (IBM Corporation, Chicago, IL, USA).

RESULTS

Similar to previous reports,^{22,27–29} the neuronal retina tissue significantly degenerated after ONT. The global loss of retinal nerve fiber bundles could be appreciated on the structural en face images of fiber bundles projected from the NFL slab through the longitudinal progression at two weeks after ONT and afterward (Fig. 2, Supplementary Fig. S1). By comparing the experimental eyes at four weeks after ONT to fellow eyes at the same time point (Supplementary Fig. S1), we can see the nerve fiber loss occurred on experimental eyes only. The perfusion of the retinal microvasculature seemed unaffected at all time points (Fig. 2). Next, we characterized the effects of ONT in detail in four ways. These include the degeneration levels of nerve fibers, the appearance and subsequent reduction of macrophage-like cells, persistence of microvasculature, and altered blood oxygen saturation.

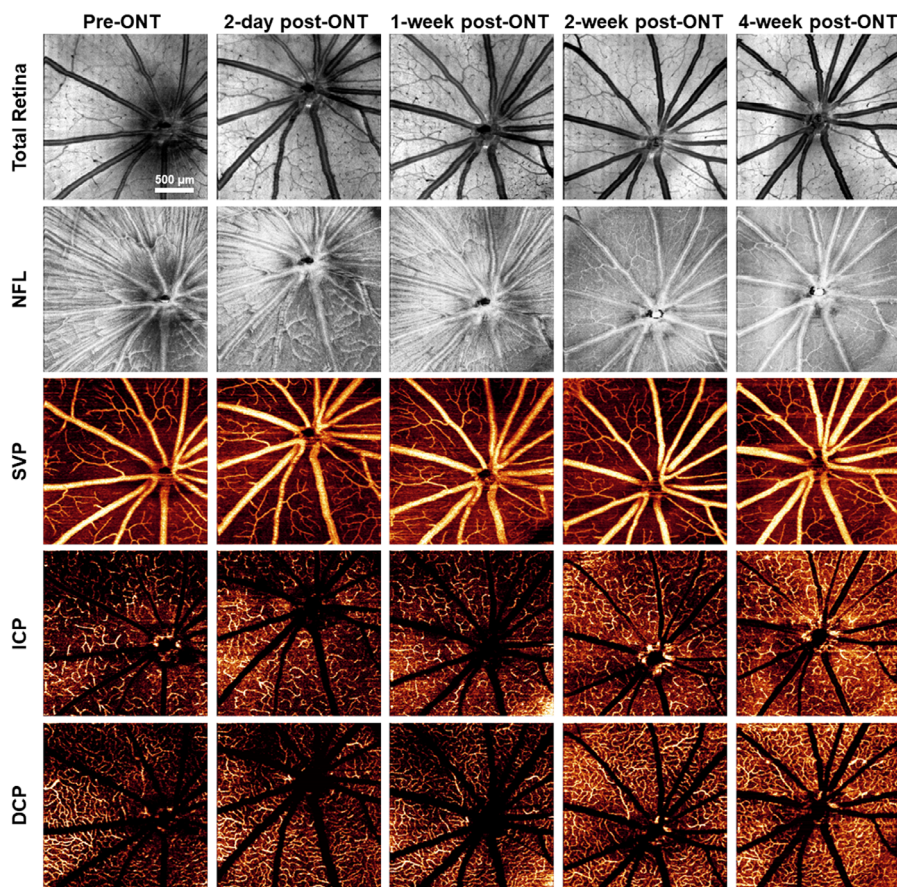


FIGURE 2. En face structural images projected from the total retina slab and NFL slab, as well as the en face angiographic images projected from SVP, ICP, and DCP plexuses in scans acquired longitudinally at timepoints of before ONT and two days, one week, two weeks, and four weeks after ONT for a representative brown Norway rat. Nerve fiber bundles were appreciated in the en face images before ONT and two days and one week after ONT, whereas they disappeared at two weeks and four weeks after ONT, indicating severe retinal neurodegeneration. However, from visual inspection, the perfusion of the retinal vasculature appears unaffected at all time points up to four weeks after ONT.

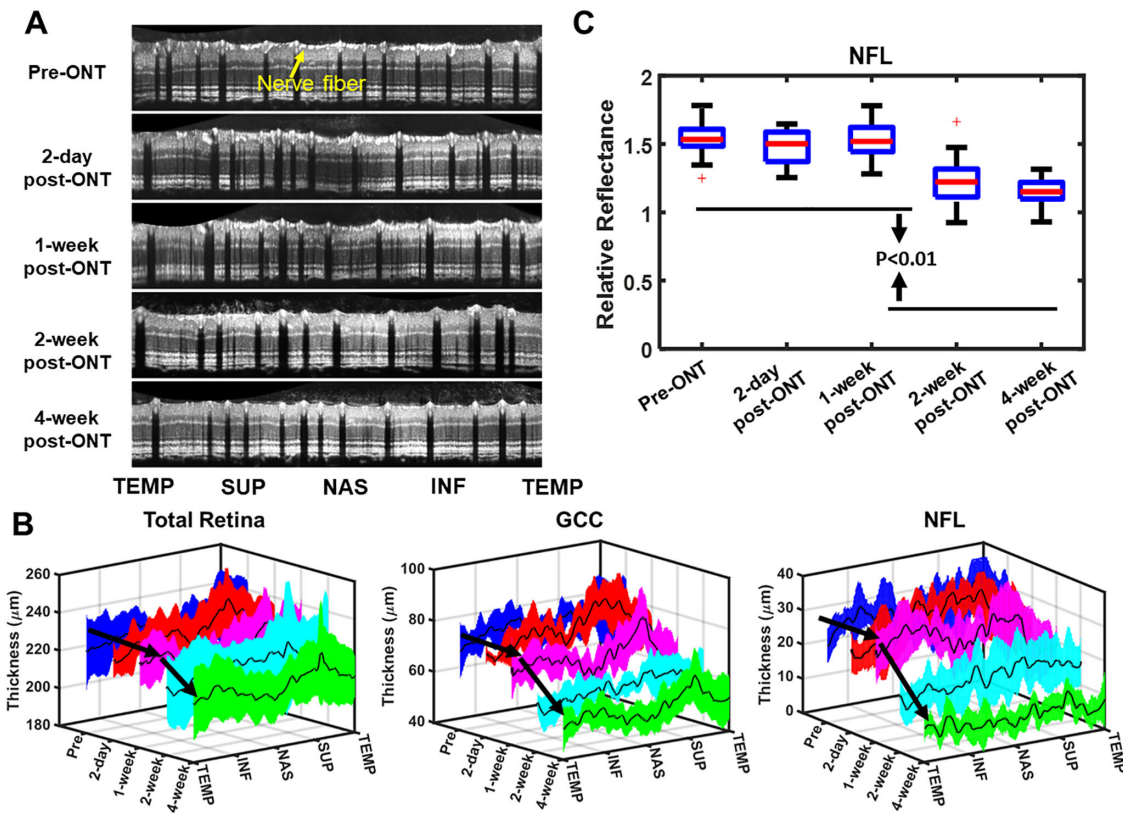


FIGURE 3. (A) Circular B-scan around optic disc acquired longitudinally at time points of before ONT and two days, one week, two weeks, and four weeks after ONT demonstrating the thinning of retinal layers, especially for the nerve fiber bundles. (B) Statistical results indicate that the thicknesses of the total retina, ganglion cell complex (GCC), and NFL were reduced in the experimental eyes after ONT, especially after two weeks after ONT. (C) Relative reflectance of NFL (defined as the ratio of the averaged OCT reflectance from the NFL slab to that from the total retina slab) for the experimental rat eyes. This was significantly decreased two weeks and four weeks after ONT, compared to baseline. TEMP, temporal; SUP, superior; NAS, nasal; INF, inferior.

Degeneration of Nerve Fibers

Nerve fiber layer bundle degeneration was visible in both the previously shown en face images and in OCT circular B-scans (Fig. 3A). As a highly scattering tissue, nerve fibers demonstrated a stronger OCT reflectance signal than the inner plexiform layer, providing distinct boundaries with the vitreous and inner plexiform layer. Corresponding to the en face images, the nerve fibers were visualized before ONT and two days and one week after ONT, but they were hardly discernable at two weeks and four weeks after ONT (Supplementary Fig. S1). Total retinal thickness demonstrated a $17.2 \mu\text{m} \pm 4.9 \mu\text{m}$ reduction between one week and two weeks after ONT. Ganglion cell complex and NFL thicknesses decreased by an average of $13\% \pm 5\%$, and $33\% \pm 14\%$ during the period (one week to two weeks after ONT) (Fig. 3B), resulting in a total of $28\% \pm 4\%$ and $70\% \pm 7\%$ decrease at four weeks after ONT when compared to baseline. Correspondingly, the reflectivity of nerve fibers was maintained until one week after ONT (1.52 ± 0.14) and decreased significantly starting from two weeks after ONT (1.23 ± 0.15), compared with that at baseline (1.54 ± 0.13) (Fig. 3C).

Macrophage-Like Cells in Vitreous

Macrophage-like cells in the vitreous slab (see definition in Fig. 1) started to appear at two days after ONT, were

present one week and two weeks after ONT, and were less evident at four weeks after ONT (Fig. 4, Supplementary Fig. S2). In contrast, these cells were not observed at baseline session.

No Change in Vessel Densities After ONT

We separated the retinal vasculature into three plexuses as SVP, ICP, and DCP. To examine the impairment in perfusion after ONT quantitatively, we calculated the vessel densities for the three plexuses (Table 1). Consistent with the visual inspection of en face OCT angiograms, there is no significant decrease in vascular densities in any of the three plexuses for the experimental eyes at four weeks after ONT.

Impaired Oxygen Saturation After ONT

Oxygen saturation significantly decreased in both arteries and veins for the experimental eyes after ONT surgery (Fig. 5A). Arterial $s\text{O}_2$ was $86\% \pm 7\%$ at baseline, $89\% \pm 5\%$ at two weeks after ONT, and decreased to $79\% \pm 9\%$ at four weeks after ONT. The venous $s\text{O}_2$ was $75\% \pm 8\%$ at baseline, $80\% \pm 4\%$ at two weeks after ONT, and decreased to $65\% \pm 12\%$ at four weeks after ONT. Fellow eyes were reimaged at four weeks and showed that arterial $s\text{O}_2$ ($87\% \pm 9\%$; $P = 0.50$) and venous oxygen saturation ($71\% \pm 10\%$; $P = 0.31$) did not change from baseline values (compared to the experimental

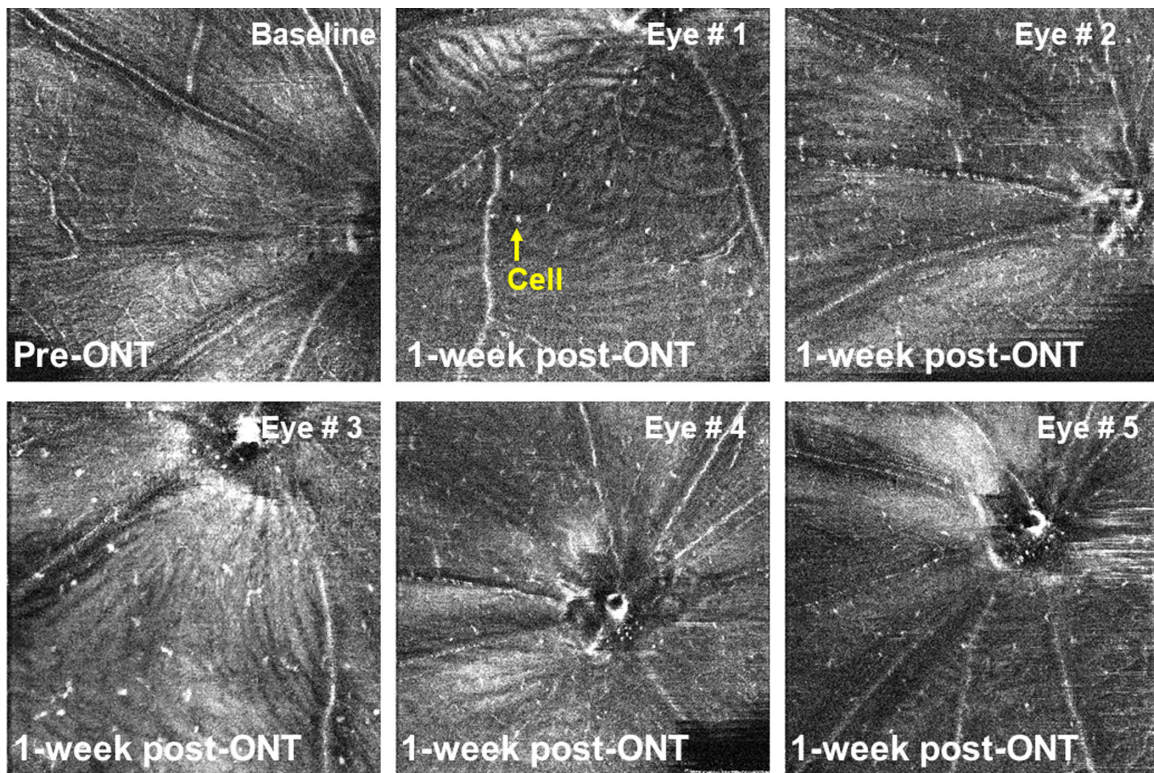


FIGURE 4. Cells appeared in rat eyes at one week after ONT, as captured by the high-resolution vis-OCT and visualized in the en face projection images of vitreous slabs. In contrast, these cells were not observed before ONT.

TABLE 1. OCTA Analysis of Vessel Densities for the Three Retinal Vascular Plexuses Demonstrated No Significant ($P > 0.05$ in Linear Mixed-Effect Model Statistics for Longitudinal Study) Impairments of Retinal Vascular Perfusion in the Rat Eyes After ONT Surgery

Imaging Session	Post-ONT					<i>P</i> Value
	Pre-ONT	Two Day	One Week	Two Weeks	Four Weeks	
Days after ONT	0	2	7	14	28	
Vessel density (%)						
SVP	26.4 ± 2.9	26.6 ± 3.7	27.1 ± 3.9	26.9 ± 4.1	27.2 ± 2.8	0.41
ICP	17.0 ± 2.5	16.7 ± 3.5	16.0 ± 3.0	15.6 ± 3.2	16.6 ± 3.2	0.92
DCP	26.6 ± 2.1	25.4 ± 4.2	25.1 ± 4.0	24.3 ± 3.3	26.9 ± 3.3	0.11

eyes at before ONT) (Fig. 5B). In the pairwise comparison, significance was observed only between the experimental eyes at four weeks after ONT compared to baseline and two weeks after ONT, and fellow eyes at four weeks (Fig. 5C).

From the representative scans shown in Figure 6, the capillary sO_2 in experimental eyes four weeks after ONT decreased significantly in the SVP (62.4 ± 3.8), as well as the DCP (64.0 ± 5.4), compared with that at baseline (SVP: 70.9 ± 11.4 ; DCP: 67.8 ± 6.7) (Table 2). By contrast, the ICP sO_2 was apparently not affected by ONT (baseline: 65.4 ± 5.3 ; ONT: 65.1 ± 4.4).

DISCUSSION

ONT in rats has been used extensively as an acute model to simulate RGC neurodegeneration in glaucoma.^{22,27–29} In this study, we explored whether this model produced both structural and angiographic evidence of damage. Previously, RGC death after ONT was confirmed using histology²² and

in vivo with OCT.^{30–32} Here, by performing high-definition vis-OCT retinal imaging, we can validate the finding in vivo and observe the progression of NFL loss longitudinally at the axial resolution of about 1 μ m. We quantified RGC thickness thinning in the ONT model more precisely owing to this high axial resolution. Our technique also allowed us to appreciate thinning of RGC axon bundles and the activation of macrophage-like cells in vivo from en face images. Additionally, our focus in this project was to investigate the response of the retinal microvasculature to ONT. We achieved this by resolving the retinal microvasculature in vivo with OCTA and calculating the vessel densities and sO_2 in all three retinal vascular plexuses.

Consistent with a previous report in mice,⁷ we found, in rats, no significant evidence of a reduction in retinal vascular perfusion, as evaluated by vessel density, up to four weeks after ONT. Although we might have seen some effect with a longer follow-up, this is unlikely, because, in the report by Smith et al.,⁷ the retinal vasculature remained unaffected up to four months after optic nerve crush. Although the

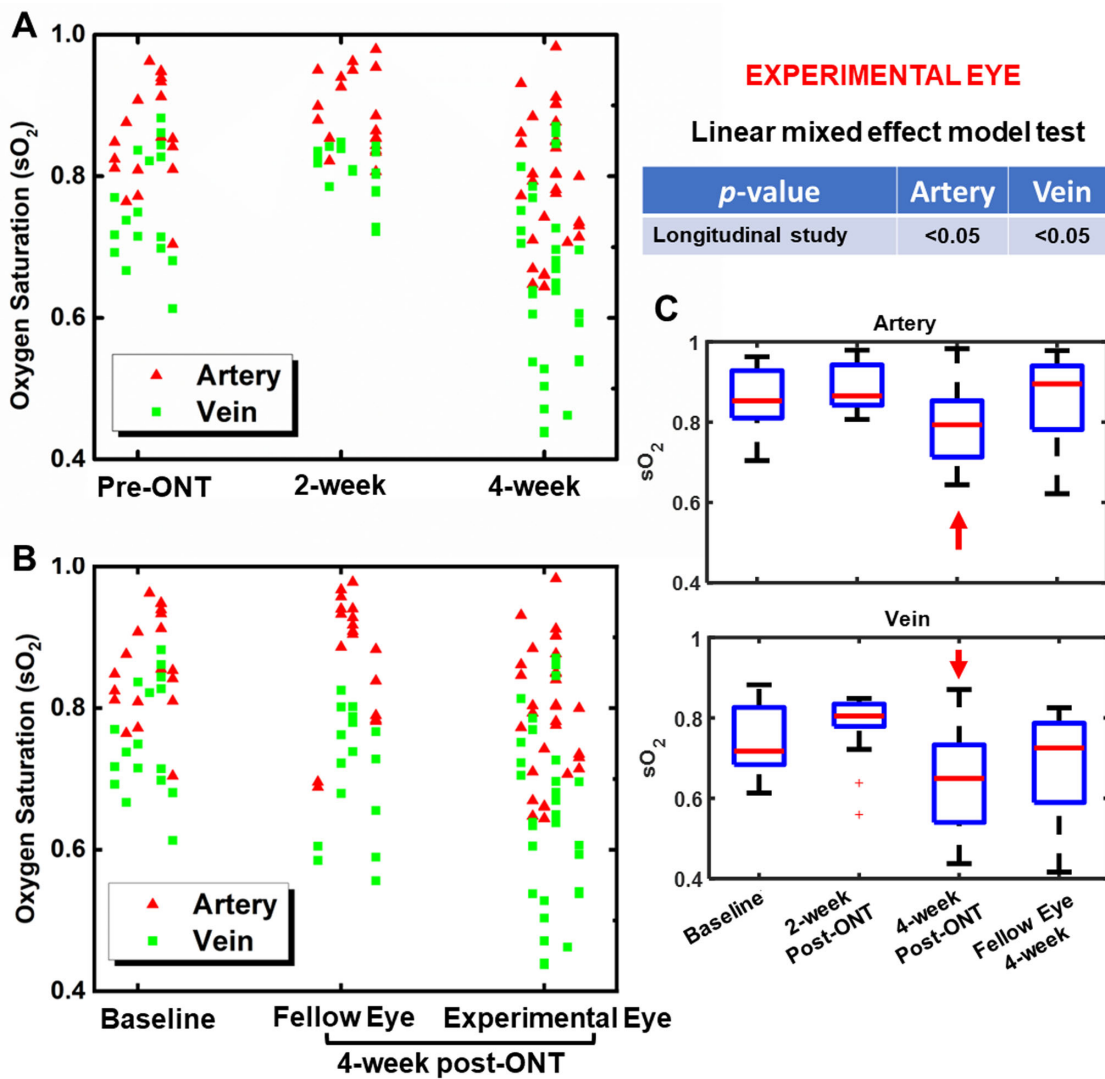


FIGURE 5. SO₂ in retinal arteries and veins for (A) experimental eyes analyzed using the linear mixed effect model demonstrated a significant decrease in both arteries and veins, (B) fellow eyes at four weeks after ONT compared to baseline and experimental eyes, (C) box plot with the significance (red arrow) observed only between the experimental eyes at four weeks after ONT to baseline, two weeks after ONT, and fellow eyes at four weeks in the pairwise comparison.

imaged retinal area might differ slightly over time, which might cause spatial variation for the vessel density analysis, the results support the finding that the retinal vascular morphology remained unchanged during the monitoring period in the ONT rat model. This finding is inconsistent with what we have observed in glaucoma patients, where both neurodegeneration and decreased vascular perfusion have been identified and appear correlated.^{2,3,33}

A potential explanation discussed by Smith et al.⁷ was the requirement of sustained oxygen supply by the neuroinflammatory response after RGC apoptosis. However, they noted that perfusion appeared unaffected for as long as four months, well beyond the duration of glial activation noted by others,³⁴ which is consistent with our observation that the increase in macrophage-like cells was diminished by four weeks. We hypothesize that one possible explanation for this inconsistency may be the different organization of the retinal vasculature between rats and humans.^{12,35,36} In humans, the NFL is relatively thicker and makes up a greater portion

of the inner retina than in rodents around the optic disc. In addition, a specific nerve fiber layer plexus (NFLP)^{30,37} is within the NFL slab (Human Panel in Fig. 7). Thus, in humans, the NFLP and NFL are closely intertwined and may contribute to a strong interplay between structural damage and vascular impairment. This would be consistent with the NFLP being the most sensitive plexus to show decreased perfusion in glaucoma patients.^{38–40} By contrast, we have observed that the rat NFL is much thinner and does not have a specific NFLP.¹² In addition, major retinal vessels, as well as the entire SVP, are located anterior to the NFL.^{12,41} Given these differences, nerve fiber layer reductions in the rat may have a relatively limited effect on vascularity, a possibility also discussed to by Smith et al.⁷

Another possible or major reason may be that the mechanism of neurodegeneration in the ONT rat model is different from that seen in human glaucoma because neurodegeneration from ONT is relatively fast whereas glaucoma is a slow, progressive neurodegenerative disorder with elevated

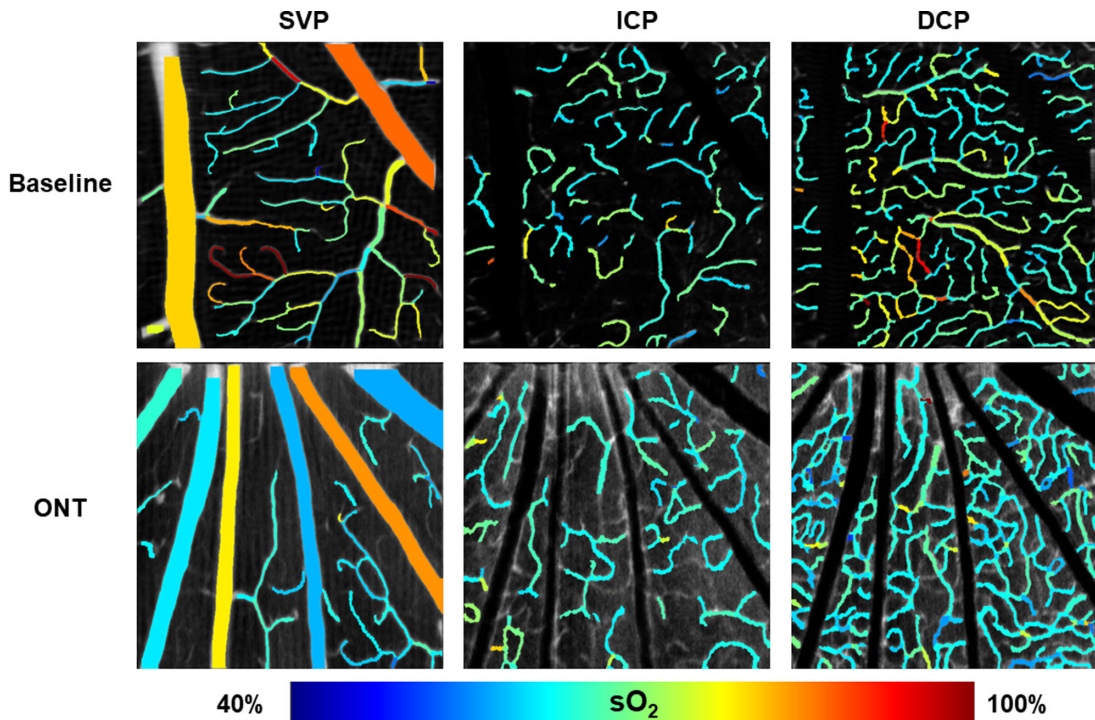


FIGURE 6. Oxygen saturation in the three retinal vascular plexuses for experimental eyes at baseline and four weeks after ONT surgery. The experimental eye demonstrated lower sO₂ in SVP and DCP after ONT surgery, indicating that reduced vascular sO₂ may be an early indicator of retinal vascular impairment.

TABLE 2. Plexus-Averaged Capillary sO₂ for SVP, ICP, and DCP at Baseline and Four Weeks After ONT and Compared With Two-Sample *t*-Test Between the Sessions

Capillary sO ₂ (%)	Baseline	ONT	Two-Sample <i>t</i> -Test <i>P</i> Value
SVP	70.9 ± 11.4	62.4 ± 3.8	<0.05
ICP	65.4 ± 5.3	65.1 ± 4.4	0.71
DCP	67.8 ± 6.7	64.0 ± 5.4	<0.05

intraocular pressure (IOP) as a primary risk factor. In addition, elevated IOP may have its own effects on retinal vascularity, in which case, reduced capillary vasculature in glaucoma might be due to more than just secondary to loss of nerve fibers. In a recent study in mice, Tao et al.⁴² found evidence of retinal ganglion cell dysfunction and retinal capillary remodeling 14 days after a single, transient IOP elevation. Although mean IOP was as high as 50 mm Hg, the reduction in capillary branches was limited to the superficial and intermediate vascular plexuses, with no effect on the deep capillaries. The potential that elevated IOP may differentially affect the retinal vasculature and possibly that of the lamina cribrosa because of laminar beam collapse or compression of the peripapillary sclera, warrants further investigation, using models with a more modest, controlled IOP exposure. If the response of the retinal vasculature varies with different insult approaches (ONT and chronic IOP elevation), this should be considered as we continue to develop animal models that better mimic glaucoma.

Interestingly, even though vessel density was unchanged four weeks after ONT, we observed a decrease in oxygen saturation in both retinal arteries and veins, as well as in

retinal capillaries in the experimental eyes, whereas saturation in the fellow eyes at that time was equivalent to pre-ONT values. Moreover, the decreases of capillary sO₂ were only observed in SVP and DCP, but not in the ICP, indicating potential plexus-dependent impairments. However, it is also possible that ICP also experienced reductions, but the vertical capillaries in ICP do not provide sufficient pixels/sampling points on two-dimensional angiograms to show the reduction, and sO₂ processing on vertical capillaries is also not as robust as that on horizontal capillaries. We included eight animals, each with unilateral ONT surgery. Based on reproducibility calibrated previously,²⁶ eight eyes would allow enough power (>0.8) to confirm the change of sO₂ at four weeks after ONT in the experimental eyes. However, we could not validate other changes (for instance, two weeks after ONT for arteries and veins) with the limited sample size. The decrease in oxygen saturation might be associated with impaired energy demand or altered neurovascular coupling after the death of RGCs. Reducing oxygenation may also precede morphological changes of blood vessels in response to environmental change. Studies with an extended monitoring period after ONT in rats, in a chronic IOP elevation model, or in glaucoma patients would be needed to compare oxygen saturation and vessel density measurements to confirm these findings and clarify possible mechanisms.

In summary, we demonstrated that vis-OCT can successfully characterize in vivo retinal damage after ONT. The retinal structure, angiography, and oximetry can all be acquired simultaneously and with high quality. Owing to this high-resolution, the vis-OCT can go beyond thickness measurement, as opposed to conventional spectral domain OCT using the infrared range.³² The emergence and

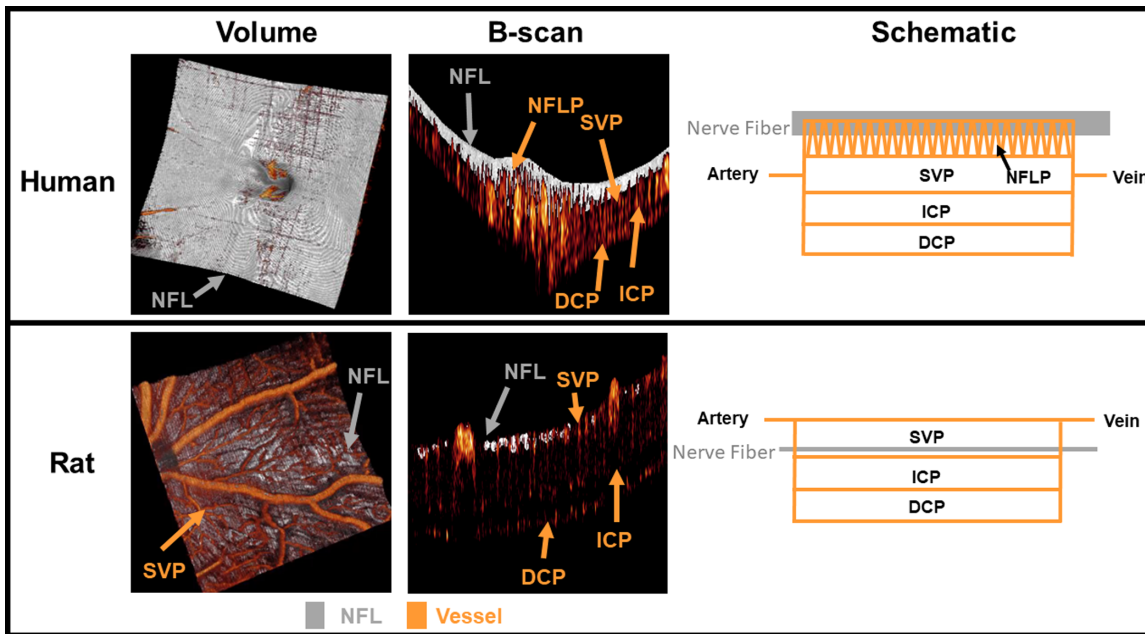


FIGURE 7. The retinal vascular (orange color) organizations with respect to NFL slab (gray color) shown in OCT/A scan volume (first column), B-scan (second column), and illustrated with schematics (third column) in humans and rats.

disappearance of cells in the vitreous were documented, accompanying this progression. We speculate these cells to be, or at least include, activated microglia after the injury²⁵ and are working on immunolabeling studies to verify this. The quantitative metrics, including thickness, reflectivity, vessel density, and oxygen saturation, provide a comprehensive delineation of the progression of retinal damage in this model. Future results, using this imaging modality in animal models with controlled elevation of IOP⁴³ that may better simulate glaucoma neurodegeneration, or in glaucoma patients, will further clarify these findings and improve our understanding of mechanisms of retinal injury in glaucoma.

Acknowledgments

Supported by grants R01 EY027833, R01 EY024544, R01 EY031394, R01 EY010145, P30 EY010572 from the National Institutes of Health (Bethesda, MD), and National Glaucoma Research (G2020168) from Bright Focus Foundation; the Career-Starter Research Grant from the Knights Templar Eye Foundation; and an unrestricted grant from Research to Prevent Blindness.

Disclosure: **S. Pi**, None; **B. Wang**, None; **M. Gao**, None; **W. Cepurna**, None; **D.C. Lozano**, None; **J.C. Morrison**, None; **Y. Jia**, Visionix/Optovue, Inc. (F, P)

References

- Kingman S. Glaucoma is second leading cause of blindness globally. *Bull World Health Organ.* 2004;82:887–888.
- Gupta N, Yücel YH. Glaucoma as a neurodegenerative disease. *Curr Opin Ophthalmol.* 2007;18:110–114.
- Yarmohammadi A, Zangwill LM, Diniz-Filho A, et al. Optical coherence tomography angiography vessel density in healthy, glaucoma suspect, and glaucoma eyes. *Invest Ophthalmol Vis Sci.* 2016;57:OCT451–OCT459.
- Bouhenni AR, Dunmire J, Sewell A, Edward DP. Animal models of glaucoma. *J Biomed Biotechnol.* 2012;2012:692609.
- Levkovich-Verbin H, Quigley HA, Martin KR, Zack DJ, Pease ME, Valenta DF. A model to study differences between primary and secondary degeneration of retinal ganglion cells in rats by partial optic nerve transection. *Invest Ophthalmol Vis Sci.* 2003;44:3388–3393.
- Magharious MM, D'Onofrio PM, Koeberle PD. Optic nerve transection: A model of adult neuron apoptosis in the central nervous system. *J Vis Exp.* 2011;(51):2241.
- Smith CA, Hooper ML, Chauhan BC. Optical coherence tomography angiography in mice: Quantitative analysis after experimental models of retinal damage. *Invest Ophthalmol Vis Sci.* 2019;60:1556–1565.
- Zhi Z, Cepurna WO, Johnson EC, Morrison JC, Wang RK. Impact of intraocular pressure on changes of blood flow in the retina, choroid, and optic nerve head in rats investigated by optical microangiography. *Biomed Opt Express.* 2012;3:2220–2233.
- Zhi Z, Cepurna W, Johnson E, Jayaram H, Morrison J, Wang RK. Evaluation of the effect of elevated intraocular pressure and reduced ocular perfusion pressure on retinal capillary bed filling and total retinal blood flow in rats by OMAG/OCT. *Microvasc Res.* 2015;101:86–95.
- Xu J, Li Y, Song S, Cepurna W, Morrison J, Wang RK. Evaluating changes of blood flow in retina, choroid, and outer choroid in rats in response to elevated intraocular pressure by 1300 nm swept-source OCT. *Microvasc Res.* 2019;121:37–45.
- Pi S, Hormel TT, Wei X, et al. Monitoring retinal responses to acute intraocular pressure elevation in rats with visible light optical coherence tomography. *Neurophotonics.* 2019;6:041104.
- Pi S, et al. Rodent retinal circulation organization and oxygen metabolism revealed by visible-light optical coherence tomography. *Biomed Opt Express.* 2018;9:5851–5862.

13. Pi S, Camino A, Wei X, et al. Retinal capillary oximetry with visible light optical coherence tomography. *Proc Natl Acad Sci.* 2020;117:11658–11666.
14. Yi J, Wei Q, Liu W, Backman V, Zhang HF. Visible-light optical coherence tomography for retinal oximetry. *Opt Lett.* 2013;38:1796–1798.
15. Shu X, Beckmann LJ, Zhang HF. Visible-light optical coherence tomography: A review. *J Biomed Opt.* 2017;22:121707.
16. Miller DA, et al. Visible-light optical coherence tomography fibergraphy for quantitative imaging of retinal ganglion cell axon bundles. *Transl Vis Sci Technol.* 2020;9:11–11.
17. Chen S, Shu X, Nesper PL, Liu W, Fawzi AA, Zhang HF. Retinal oximetry in humans using visible-light optical coherence tomography. *Biomed Opt Express.* 2017;8:1415–1429.
18. Song W, Shao W, Yi W, et al. Visible light optical coherence tomography angiography (vis-OCTA) facilitates local microvascular oximetry in the human retina. *Biomedical Optics Express.* 2020;11:4037–4051.
19. Rubinoff I, Miller DA, Kuranov R, et al. Balanced-detection visible-light optical coherence tomography. *bioRxiv.* 2021;2021–2106.
20. Zhang T, Kho AM, Zawadzki RJ, Jonnal RS, Yiu G, Srinivasan VJ. Visible light OCT improves imaging through a highly scattering retinal pigment epithelial wall. *Opt Lett.* 2020;45:5945–5948.
21. Pi S, Camino A, Zhang M, et al. Angiographic and structural imaging using high axial resolution fiber-based visible-light OCT. *Biomed Opt Express.* 2017;8:4595–4608.
22. Nadal-Nicolás FM, Jiménez-López M, Sobrado-Calvo P, et al. Brn3a as a marker of retinal ganglion cells: Qualitative and quantitative time course studies in naive and optic nerve-injured retinas. *Invest Ophthalmol Vis Sci.* 2009;50:3860–3868.
23. Wojtkowski M, Srinivasan VJ, Ko TH, Fujimoto JG, Kowalczyk A, Duker JS. Ultrahigh-resolution, high-speed, Fourier-domain optical coherence tomography and methods for dispersion compensation. *Opt Express.* 2004;12:2404–2422.
24. Guo Y, Camino A, Zhang M, et al. Automated segmentation of retinal layer boundaries and capillary plexuses in wide-field optical coherence tomographic angiography. *Biomed Opt Express.* 2018;9:4429–4442.
25. Wohl SG, Schmeer CW, Witte OW, Isenmann S. Proliferative response of microglia and macrophages in the adult mouse eye after optic nerve lesion. *Invest Ophthalmol Vis Sci.* 2010;51:2686–2696.
26. Pi S, Camino A, Cepurna W, et al. Automated spectroscopic retinal oximetry with visible-light optical coherence tomography. *Biomed Opt Express.* 2018;9:2056–2067.
27. Sánchez-Migallón M, Valiente-Soriano FJ, Salinas-Navarro M, et al. Nerve fibre layer degeneration and retinal ganglion cell loss long term after optic nerve crush or transection in adult mice. *Exp Eye Res.* 2018;170:40–50.
28. Ahmed Z, Suggate EL, Logan A, Berry M. Retinal ganglion cell survival and axon regeneration after optic nerve transection is driven by cellular intravitreal sciatic nerve grafts. *Cells.* 2020;9:1335.
29. Li H-Y, Ruan Y-W, Ren C-R, Cui Q, So K-F. Mechanisms of secondary degeneration after partial optic nerve transection. *Neural Regen Res.* 2014;9:565.
30. Chauhan BC, Stevens KT, Levesque JM, et al. Longitudinal in vivo imaging of retinal ganglion cells and retinal thickness changes following optic nerve injury in mice. *PloS One.* 2012;7:e40352.
31. Rovere G, Nadal-Nicolás FM, Agudo-Barriuso M, et al. Comparison of retinal nerve fiber layer thinning and retinal ganglion cell loss after optic nerve transection in adult albino rats. *Invest Ophthalmol Vis Sci.* 2015;56:4487–4498.
32. Choe TE, Abbott CJ, Piper C, Wang L, Fortune B. Comparison of longitudinal in vivo measurements of retinal nerve fiber layer thickness and retinal ganglion cell density after optic nerve transection in rat. *PloS One.* 2014;9:e113011.
33. Takusagawa HL, Liu L, Ma KN, et al. Projection-resolved optical coherence tomography angiography of macular retinal circulation in glaucoma. *Ophthalmology.* 2017;124:1589–1599.
34. Nadal-Nicolás FM, Jiménez-López M, Salinas-Navarro M, Sobrado-Calvo P, Vidal-Sanz M, Agudo-Barriuso M. Microglial dynamics after axotomy-induced retinal ganglion cell death. *J Neuroinflammation.* 2017;14:1–15.
35. Nesper PL, Fawzi AA. Human parafoveal capillary vascular anatomy and connectivity revealed by optical coherence tomography angiography. *Invest Ophthalmol Vis Sci.* 2018;59:3858–3867.
36. Campbell J, Zhang M, Hwang TS, et al. Detailed vascular anatomy of the human retina by projection-resolved optical coherence tomography angiography. *Sci Rep.* 2017;7:1–11.
37. Jia Y, Simonett JM, Wang J, et al. Wide-field OCT angiography investigation of the relationship between radial peripapillary capillary plexus density and nerve fiber layer thickness. *Invest Ophthalmol Vis Sci.* 2017;58:5188–5194.
38. Liu L, Edmunds B, Takusagawa HL, et al. Projection-resolved optical coherence tomography angiography of the peripapillary retina in glaucoma. *Am J Ophthalmol.* 2019;207:99–109.
39. Chen A, Liu L, Wang J, et al. Measuring glaucomatous focal perfusion loss in the peripapillary retina using OCT angiography. *Ophthalmology.* 2020;127:484–491.
40. Liu L, Takusagawa HL, Greenwald MF, et al. Optical coherence tomographic angiography study of perfusion recovery after surgical lowering of intraocular pressure. *Sci Rep.* 2021;11:1–8.
41. Pi S, Hormel TT, Wei X, Cepurna W, Morrison JC, Jia Y. Imaging retinal structures at cellular-level resolution by visible-light optical coherence tomography. *Opt Lett.* 2020;45:2107–2110.
42. Tao X, Sigireddi RR, Westenskow PD, Channa R, Frankfort BJ. Single transient intraocular pressure elevations cause prolonged retinal ganglion cell dysfunction and retinal capillary abnormalities in mice. *Exp Eye Res.* 2020;201:108296.
43. Morrison JC, Cepurna WO, Tehrani S, et al. A period of controlled elevation of IOP (CEI) produces the specific gene expression responses and focal injury pattern of experimental rat glaucoma. *Invest Ophthalmol Vis Sci.* 2016;57:6700–6711.